Journal of Power Sources 246 (2014) 788–799

Contents lists available at ScienceDirect

Journal of Power Sources

journal homepage: www.elsevier.com/locate/jpowsour

Effect of manufacturing process sequence on the corrosion resistance characteristics of coated metallic bipolar plates

Ender Dur [a,b], Ömer Necati Cora [a,c], Muammer Koç [a,d,*]

[a] NSF I/UCRC Center for Precision Forming (CPF), Richmond, VA, USA
[b] Istanbul Gas Distribution Company (IGDAS), 34060 Istanbul, Turkey
[c] Karadeniz Technical University, 61080 Trabzon, Turkey
[d] Istanbul Sehir University, 34660 Istanbul, Turkey

HIGHLIGHTS

- Forming-coating sequence effects on the corrosion resistance of BPPs were examined.
- Two process sequence, forming methods, and PD-PS corrosion test methods were used.
- Corrosion performance of coating materials on BPPs was ZrN > CrN > TiN > uncoated.
- It was also found that thicker coating increased the corrosion resistance.
- Coating before manufacturing does not always decrease the corrosion resistance.

ARTICLE INFO

Article history:
Received 30 May 2013
Received in revised form
25 July 2013
Accepted 8 August 2013
Available online 19 August 2013

Keywords:
Bipolar plate
Corrosion
Coating
Process sequence effect
Hydroforming
Stamping

ABSTRACT

Metallic bipolar plate (BPP) with high corrosion and low contact resistance, durability, strength, low cost, volume, and weight requirements is one of the critical parts of the PEMFC. This study is dedicated to understand the effect of the process sequence (manufacturing then coating vs. coating then manufacturing) on the corrosion resistance of coated metallic bipolar plates. To this goal, three different PVD coatings (titanium nitride (TiN), chromium nitride (CrN), zirconium nitride (ZrN)), with three thicknesses, (0.1, 0.5, 1 μm) were applied on BPPs made of 316L stainless steel alloy before and after two types of manufacturing (i.e., stamping or hydroforming). Corrosion test results indicated that ZrN coating exhibited the best corrosion protection while the performance of TiN coating was the lowest among the tested coatings and thicknesses. For most of the cases tested, in which coating was applied before manufacturing, occurrence of corrosion was found to be more profound than the case where coating was applied after manufacturing. Increasing the coating thickness was found to improve the corrosion resistance. It was also revealed that hydroformed BPPs performed slightly better than stamped BPPs in terms of the corrosion behavior.

1. Introduction

Metallic bipolar plates (BPPs) must be corrosion resistant since PEMFC environment is acidic and humid [1]. In order to improve the corrosion resistance of metallic BPP and meet the DOE (Department of Energy, USA) target for corrosion current density of lower than 1 μA cm^{-2} [2], surface treatments such as coatings are extremely important [1]. These coatings need to be electrically conductive and corrosion resistant. There are various coating material alternatives such as polymers, noble metals, metal nitrides, metal carbides, etc. that can be applied on metallic plates to satisfy the DOE target [3]. Carbon based or metal-based coating materials are widely reported in literature [4]. Studies available in the literature mostly preferred the physical vapor deposition (PVD) method for coating of metallic materials against corrosion [5–7].

Garcia and Smit selected the polypyrrole coated SS 304 sheet sample to study the corrosion endurance of the coating. The electrodeposition method was employed to cover a 1 cm^2 surface area of the substrate material with diverse amount of polypyrrole. They observed that polypyrrole improved the corrosion behavior of the sample, however; determining the optimum coating composition was required to achieve long-term stability in PEMFC [8]. Wang and Northwood also examined the effect of polypyrrole coating material on the corrosion behavior of SS 316L. Galvanostatic and cyclic

* Corresponding author. Istanbul Sehir University, 34660 Istanbul, Turkey.
E-mail address: koc.muammer@gmail.com (M. Koç).

0378-7753/$ – see front matter © 2013 Elsevier B.V. All rights reserved.
http://dx.doi.org/10.1016/j.jpowsour.2013.08.036

voltammetric processes were used to deposit the coating on the 2.25 cm^2 surface area [9]. It was concluded that the positive effects of polypyrrole coating on corrosion resistance was similar to that in Garcia and Smit. Ren and Zeng combined the polypyrrole with a polyaniline to have a bilayer composite coating material in their study. They reported that composite coating was better than single polypyrrole coating in terms of the corrosion characteristic [10]. Joseph et al. tested two polymer-coating materials (polypyrrole, polyaniline) in their work. They supported the previous results by others regarding with the good corrosion behaviors of these coatings [11]. Morks et al. reported promising corrosion resistance results for plasma-sprayed W-Ni coatings [12]. Another work by Lee and Lim investigated a polymer composite of polyamide-imide filled with carbon black by determining the optimum carbon black content for BPP's better corrosion and lower contact resistance [13].

Lee et al. compared the corrosion resistance SS 316L and AA 5052 sheets that were shaped into the BPPs via CNC machining or EDM. The AA 5052 sheet was coated with the YZU001 diamond-like coating by means of physical vapor deposition (PVD) technique while the SS 316L used as uncoated. Although the SS 316L was uncoated, it demonstrated higher corrosion resistance than the coated AA 5052. Nevertheless, the aluminum possessed lower contact resistance value compared to SS 316L sheet [14].

Similar to many other researchers, Yu et al. selected the SS 316L material to test the coating influence on corrosion behavior. Authors coated the SS 316L sample with a tantalum (Ta) coating through PVD process. Comparison between uncoated and coated SS 316L samples disclosed that the Ta coating improved the corrosion resistance of the sample [6].

Jung et al. manufactured the BPPs from the titanium block with the dimension of 7.5 × 7.5 × 1.2 cm. The BPP had serpentine type flow-fields with 1 mm-deep channels, and 5 cm^2 surface area. The BPP, covered with 1 μm gold coating, increased the unit cell performance by blocking the oxidation forming on surface [15]. Similarly, Kumar et al. noted that gold coatings provide excellent corrosion protection for metallic BPPs even with nanometer thickness level (10 nm) [1]. In another study by Yun, firstly the 0.1 μm titanium or nickel, and then the 1 μm and 2 μm gold was deposited on the surface of SS 316L blanks by electron-beam-evaporation process. Results indicated the gold-coated samples as appropriate BPP candidates in PEMFC [16].

Yoon et al. studied several substrates (SS 304, SS 310, SS 316) and coating materials (Ti, Zr, ZrN, ZrNb, ZrNAu, 2 nm–10 nm–1 μm-thick gold) through PVD coating process. Both anode and cathode environments of PEMFC were simulated in polarization tests for coated metal samples with a 3 cm^2 surface area. According to the corrosion test results, Zr, ZrN, ZrNb, ZrNAu and 10 nm-thick gold-coated samples met the DOE target in the anode side while only the Zr coated sample reached the DOE target in the cathode side. Moreover, thicker coating materials were found to demonstrate higher corrosion-resistance [17]. Barranco et al. reported the corrosion behaviors of single chromium nitride (CrN) and multilayer zirconium-chromium nitride coatings on the AA 5083 alloy. Coatings were applied by means of the cathodic arc evaporation physical vapor deposition (CAE-PVD) method on one side of the samples. Short-term corrosion tests confirmed the suitability of these coatings and the PVD coating method for aluminum plates [7].

Jeong et al. and Feng et al. experimented on Ni–Cr rich-coating-layers and reported that the amount of Ni–Cr content should be optimized to accomplish expected corrosion resistance for SS 316L BPP in PEMFC [18,19]. Barronco et al. investigated the BPPs of CrN-coated AA 5083 by using three different coating thicknesses (3, 4, 5 μm). Although CrN coated AA 5083 displayed better corrosion resistance compared to uncoated aluminum, it may not be appropriate for BPP since some corrosion pitting holes were detected on the surface after corrosion test [20]. On the other hand, Tian and Fu et al. also researched CrN film on the SS 316L BPP material and their results noted promising features of CrN in terms of electrochemical stability and interfacial electrical conductivity [21–23].

Wang et al. utilized TiN coating on the SS 316L with the PVD coating technique. Two electrochemical (potentiodynamic and impedance) test methods were used to evaluate the corrosion resistance. Approximately 15 μm-thick TiN coating was found not to be a good coating option for BPP since it incorporated pinholes [24]. Zhang et al. preferred SS 304 substrate material as BPP to observe the corrosion-resistance performance of TiN coating. Different from Wang et al., Zhang et al. implemented two different coating processes: pulsed bias arc ion plating (PBAIP) and magnetron sputtering (MS) in their study. The results specified Ti_2N/TiN multilayer coating as the corrosion resistant coating for BPP [25].

Eriksson at al. studied the formability and corrosion behavior of TiN-coated AISI 304 stainless steel. Corrosion tests were conducted after the forming process. The authors reached following conclusions;

1 Hard coating did not prevent the formability of the coated sheet,
2 Although some cracks were observed under the microscope after the manufacturing process, uniform coating color was still seen on the surface,
3 With higher coating thicknesses, cracks numbers declined,
4 Forming process reduced the corrosion resistance of TiN coated sample, however, TiN coated sample showed better corrosion protection than the uncoated sample as expected [26].

There are several other studies on performance of TiN, CrN, TiAlN, CrN–Ti, TiC and multilayer TiN/CrN coatings applied mostly on SS 316L substrates [27–35].

Fu et al. studied three different carbon-based films (C, C–Cr, and C–Cr–N films) as coating materials for SS 316L BPP. Only the C–Cr film coated sample was found to be suitable in PEMFC conditions according to potentiodynamic and potentiostatic test results [36]. Feng et al. also coated SS 316L coupons with carbon film. Amorphous-carbon (a-C) coating was processed via close field unbalanced magnetron sputter ion plating (CFUBMSIP) technique. They concluded that a-C could be an alternative coating material for the metallic BPPs [37]. The positive effects of the carbon-based coatings on the metallic BPP in corrosion resistance were repeated by Fukutsuka et al. and Lee et al. [38,39].

Another way to improve corrosion resistance and lower the contact resistance of BPP is surface modification methods [40]. Lee et al. applied surface treatment on the SS 316L specimen to obtain a better surface quality resulting in high corrosion resistance and low contact resistance. They observed that since the surface became smoother after treatment, the sample was developed into a more corrosion resistant material [41]. Cho et al. performed the chromizing surface modification on SS 316L material by pack cementation method. This treatment improved the corrosion protection feature of the sample in short-term tests, while no development on the corrosion behavior was seen after 10 h-long-term test [42]. In addition, chromized steels were recommended in terms of the electrochemical stability in literature [43–46]. Another option to coat BPP is niobium, which was reported in literature with promising anti-corrosion performance [47–49].

All of these studies showed that corrosion resistance target can be satisfied, however; in most of them, both corrosion and contact resistance targets were not satisfied at the same time. The contact resistance target level set by DOE is less than 10 mΩ m^2 at

140 N mm^{-2}. It is essential to coat or modify the substrate material in order to meet both corrosion and contact resistance targets. Therefore, there are ongoing efforts to find and develop suitable substrate-coating material combinations that provide sufficiently high corrosion, and low contact resistance for BPPs. Multi-faceted investigations from different perspectives including the effect of process sequence (coating, then forming of BPPs vs. forming, then coating) on corrosion and contact resistance performance of BPPs may reveal important information to satisfy the requirements.

There are two different possible sequences for manufacturing of coated BPPs: (1) coating is applied on the sheet material, and then it is formed (shaped by manufacturing) into the BPP with micro-channels of flow field; (2) BPP is formed first, and then coated. It is assumed that the process sequence affects the BPP corrosion performance since surface conditions, thus manufacturing, have influence on corrosion resistance characteristics. If the coating is applied onto blanks before manufacturing process, it offers several advantages such as improved product quality, reduced production cost, and shorter and automated processing cycle, reduction of production scrap and energy savings [50].

As summarized above, this field needs to research more to find out the effect of manufacturing and the process sequence on coatings and corrosion resistance for PEMFC BPPs characteristics. This study, therefore, is dedicated to the experimental investigations on the process sequence effect on the corrosion resistance of metallic BPPs manufactured using stamping and hydroforming processes. Previous studies by the authors examined the corrosion resistance of metallic BPPs that were coated after forming [51]. Current investigation, however, aims revealing the corrosion resistance performance of coated BPPs produced with two different forming methods (stamping and hydroforming) and above-mentioned two different process sequences. Subsequent sections present the experimental conditions, corrosion resistance test results, and conclusions.

2. Experimental procedure

Two manufacturing methods, namely hydroforming and stamping, were used to produce metallic BPPs. SS 316L (Brown Metals Co., Rancho Cucamonga, CA, USA) sheet blanks with 51 μm thickness were used as BPP substrate material. Titanium Nitride (TiN), Chromium Nitride (CrN), Zirconium Nitride (ZrN), at three different thicknesses (0.1, 0.5, 1 μm) were selected as surface coatings. Two different process sequences were followed: 1) Sheet blanks were formed to BPPs first, and then coated, 2) Sheet blanks were coated first, and then formed. Those two forming-coating sequences will be referred as (1) formed-coated and (2) coated-formed hereafter. In some figures, first coated and then formed samples were denoted with the letter C (i.e. C-hydroformed instead of coated-hydroformed) as well. Fig. 1 shows coated BPP images before and after manufacturing.

Coating process for sheet blanks and formed BPPs were performed by Tanury Industries (Tanury Industries Co., Lincoln, RI, USA). The details of PVD coating process can be found elsewhere [17,51].

After BPPs were manufactured, they were exposed to potentiodynamic (PD) and potentiostatic (PS) corrosion tests. Since the corrosion formation in the cathode side is known to be faster and more severe than that of in the anodic side as reported in several studies [32,33,37], only O_2 gas was bubbled into the solution of the corrosion test cell to simulate the cathodic condition of the PEMFC. Blank samples (coated and uncoated) were also included in corrosion tests for comparison purposes. Extensive scanning electron microscopy investigations were performed on the micro-channel peaks of the BPPs before and after PS corrosion tests using JSM-5610LV SEM (JEOL Ltd., Tokyo, Japan). EDX analyses were also performed on some coated samples to determine the chemical properties of the surface using Hitachi FE-SEM Su-70 (Hitachi, Ltd., Japan). Statistical analyses were performed by means of ANOVA technique on the PD corrosion test results to reveal the significance of process variables.

2.1. Manufacturing of BPPs

Stamping and hydroforming processes were implemented for manufacturing of BPPs with several micro-channels. Hydroforming is noted for better formability, channel height, and uniform thickness distribution as well as decreased tool cost by using only one die [52–55]. Stamping process, on the other hand, provides faster cycle time; thus, suitable for mass production [53,56]. Forming equipment used for both hydroforming and stamping processes were given in Fig. 2a and b.

Based on previous experience [57–60] force level of 200 kN, and punch speed of 1 mm s^{-1} in stamping; maximum hydroforming pressure of 40 MPa, and pressure rate of 1 MPa s^{-1} in hydroforming were chosen as manufacturing parameters to fabricate metallic BPPs.

2.2. Corrosion tests

Manufactured BPPs were exposed to corrosive environment to assess their corrosion resistance. Two commonly referred electrochemical corrosion test methods in literature [11,36,39,43,44]

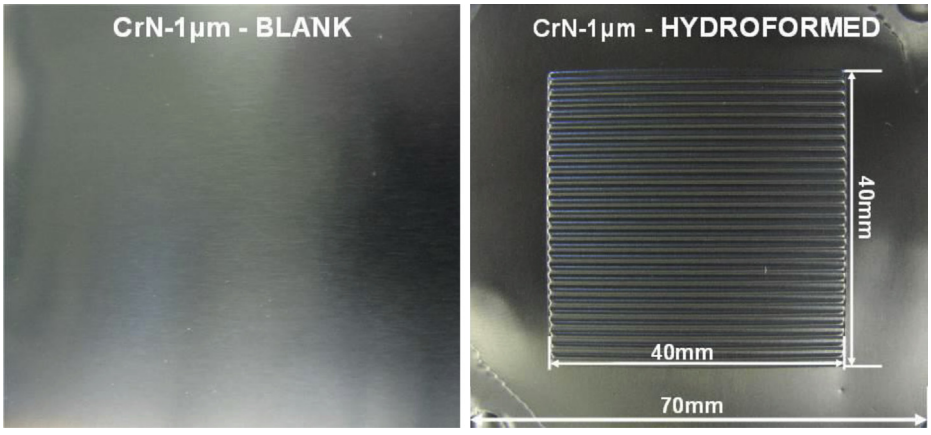

Fig. 1. Coated blank and coated-hydroformed samples.

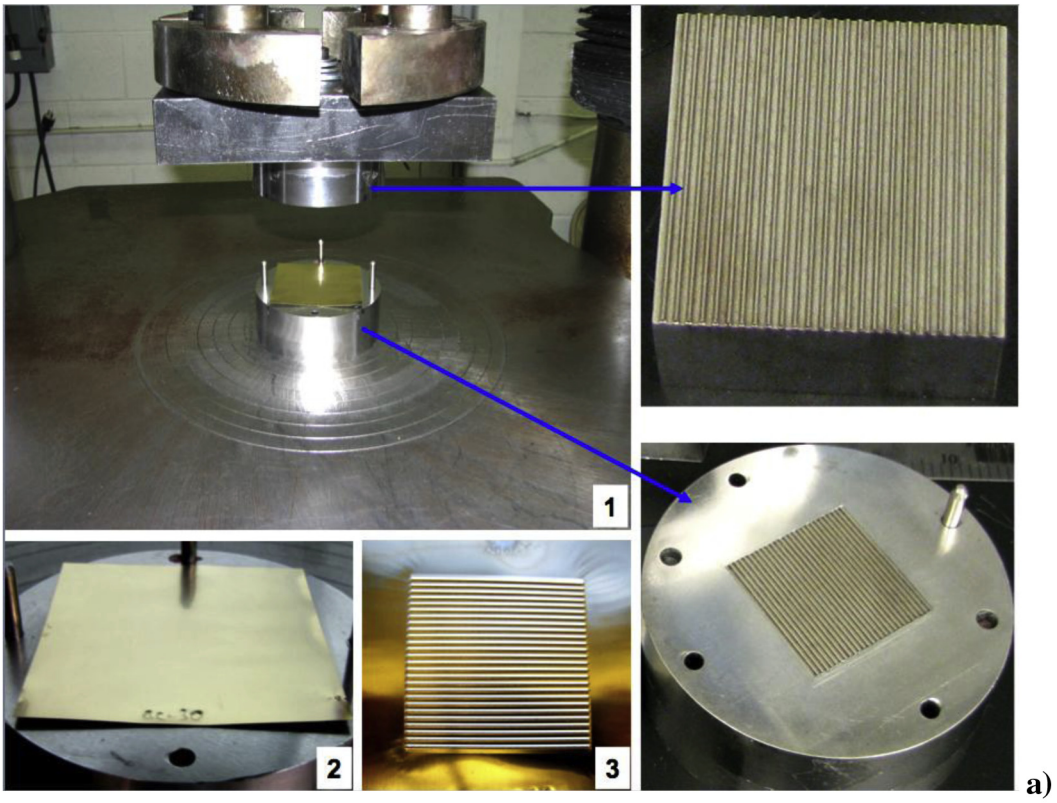

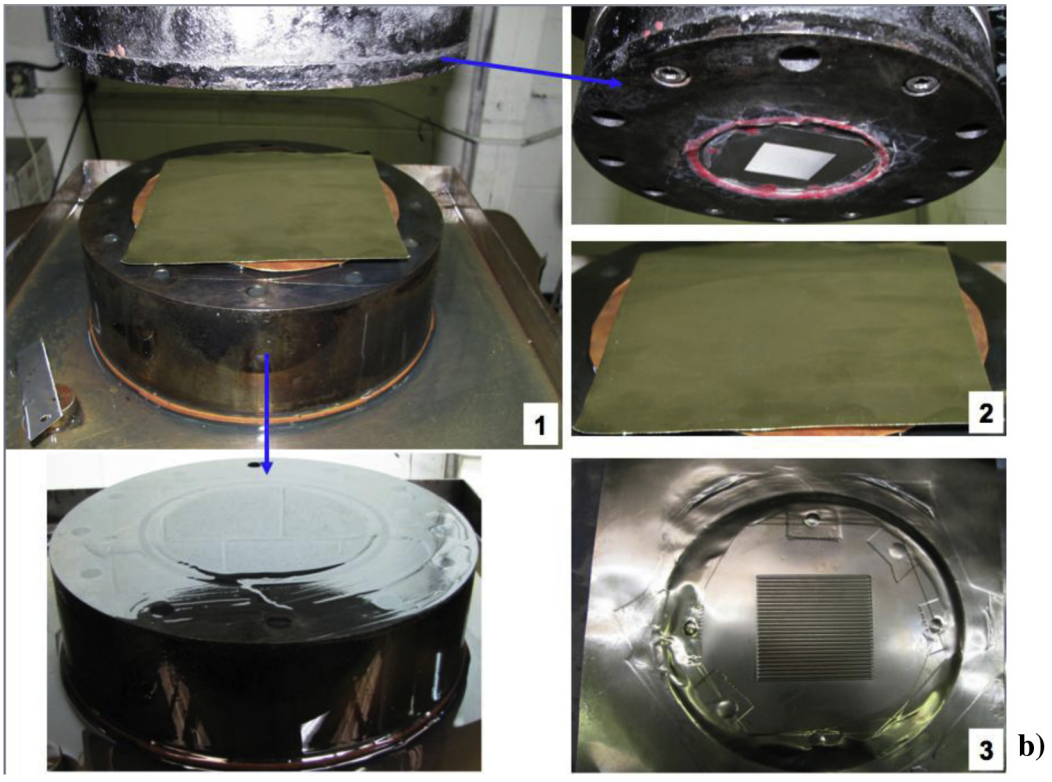

Fig. 2. Manufacturing test setups: a) 1-stamping setup, 2-coated blank sample, 3-stamped sample, b) 1-hydroforming setup, 2-coated blank sample, 3-hydroformed sample.

namely potentiodynamic (PD) and potentiostatic (PS) tests, were exploited in this investigation. At least three samples from each case were tested in PD conditions, whereas only one sample was used in long-term PS tests due to prolonged test durations. Corrosion test setup consisted of a working electrode (BPP sample), a graphite counter electrode, an Ag/AgCl reference electrode and acidic solution tank with a gas bubbler at the bottom. Acidic solution providing the PEMFC atmosphere was the 0.5 M H_2SO_4 (sulfuric acid). Corrosion cell was placed into a furnace and heated up to 80 °C to simulate the PEMFC working temperature condition. Before corrosion test, uncoated samples were cleaned in an ultrasonic acetone bath for 30 min while coated samples were exposed to this process for shorter duration to prevent the unexpected effects of ultrasonic bath and acetone. BPP surface was selectively protected by exposing only channeled area (40 × 40 mm) to the corrosion effect.

Potential range of −1.2 to 0.8 V at a rate of 1 mV s^{-1} was applied in PD corrosion tests. Polarization curves were transformed to the corrosion current density (I_{corr}) data by Tafel analysis method. PS corrosion tests, on the other hand, were performed at a constant potential of 0.6 V with the O_2 purge for 3 h. Both corrosion tests were managed via Solartron 1287 Electrochemical Interface potentiostat device (Solartron Analytical, Oak Ridge, TN, USA).

Corrosion current density values (I_{corr}) were used to evaluate the corrosion behavior of the manufactured metallic BPPs. Lower corrosion current density represents the higher corrosion resistance [61]. Detailed information on corrosion test procedure is available in previous studies by authors [57,59].

3. Results and discussion

3.1. Potentiodynamic test results

Fig. 3 illustrates PD corrosion test results with O_2 gas for all uncoated, coated blank and formed samples that were coated prior to manufacturing (coated-formed). Besides, the average of corrosion current densities for each coating group, which includes two different forming-coating sequences, was summarized in Table 1.

Ranking of corrosion resistance for BPPs from high to low was based on the low-to-high corrosion current density values. As seen in Fig. 3, the order of corrosion current density values from high to low was found to be in the order of ZrN > CrN > TiN > Uncoated blank for most cases. These results implied that coating material had a significant impact on the corrosion characteristics of the metallic BPPs, as expected. Coating thickness was another factor, which alters the current density value of the sample as previously reported in literature [26,27]. Current research confirmed previous findings as it was noted that thicker the coating the higher corrosion resistance. 1 μm-thick-coated samples showed the best corrosion resistance while 0.1 μm-thick-coated samples resulted in the worst corrosion resistance, regardless of process sequence (formed-coated vs. coated-formed). This fact was valid for each coating group except the hydroformed samples case. 0.1 μm-thick-TiN-coated hydroformed BPPs yielded lower corrosion current density than that for 0.5 μm-thick-TiN-coated hydroformed BPPs among the formed-coated type samples. The same trend was observed for coated-formed group samples, as well. Another important remark from PD corrosion tests was that the blank (unformed-coated) samples displayed better corrosion behavior when compared to both formed-coated and coated-formed groups, in general.

It was concluded that manufacturing parameters influenced the corrosion resistance of metallic BPPs. These results also showed the importance of testing of manufactured BPPs along with the blank samples rather than testing only the bulk or blank sheet samples in corrosion studies to gain comprehensive information.

As mentioned above, ZrN coating material characterized superior corrosion endurance among not only blank and formed-coated groups but also among coated-formed groups. According to the previous work that includes the formed-coated BPP corrosion test results, ZrN coated blank and formed samples met the DOE target regarding the corrosion rate of metallic BPPs except two cases. Stamped and hydroformed-0.1 μm-thick-ZrN-coated BPPs bore higher corrosion density values than the DOE target value of 1 μA cm^{-2} in cathodic condition. In the group of coated-formed BPPs as portrayed in Fig. 3, on the other hand, only hydroformed BPPs with 1 μm-thick-ZrN coating satisfied this DOE target.

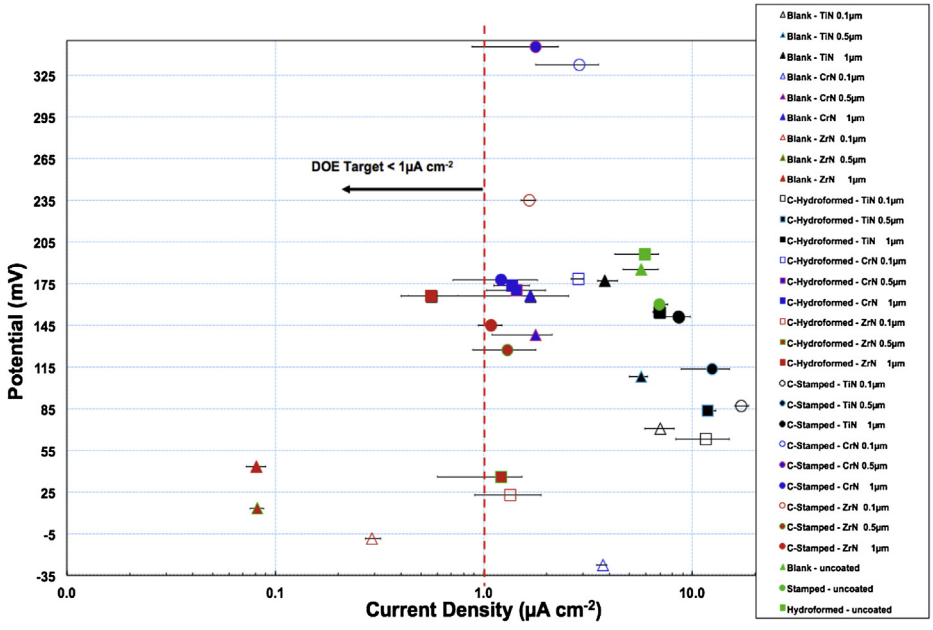

Fig. 3. PD corrosion test results for coated and uncoated blanks; uncoated hydroformed, stamped samples; and all other coated-formed samples.

Table 1
Average corrosion current density data for formed-coated and coated-formed BPPs.

Process – coating – thickness (μm)	I_{corr} (μA cm^{-2}) formed-coated	I_{corr} (μA cm^{-2}) coated-formed	Process – coating – thickness (μm)	I_{corr} (μA cm^{-2}) formed-coated	I_{corr} (μA cm^{-2}) coated-formed
Hydroforming – TiN -0.1	10.19	11.58	Stamping – TiN – 0.1	7.80	17.13
Hydroforming – TiN -0.5	10.69	11.89	Stamping – TiN – 0.5	7.62	12.44
Hydroforming – TiN – 1	6.56	6.94	Stamping – TiN – 1	5.89	8.60
Hydroforming – CrN -0.1	3.32	2.85	Stamping – CrN – 0.1	3.47	2.87
Hydroforming – CrN -0.5	2.67	1.44	Stamping – CrN – 0.5	2.66	1.78
Hydroforming – CrN – 1	1.79	1.36	Stamping – CrN – 1	1.70	1.22
Hydroforming – ZrN – 0.1	1.30	1.34	Stamping – ZrN – 0.1	1.48	1.66
Hydroforming – ZrN – 0.5	0.72	1.21	Stamping – ZrN – 0.5	0.81	1.31
Hydroforming – ZrN – 1	0.33	0.56	Stamping – ZrN – 1	0.48	1.08

Moreover, PD corrosion test results indicated that TiN coating material demonstrated an adverse impact on the corrosion resistance in most cases for formed-coated BPPs. Similar conclusions were obtained for coated-formed BPPs, too.

In order to assess the effect of manufacturing process sequence (i.e. formed-coated and coated-formed) on the corrosion resistance of BPPs in detail, the following subsections were devoted to comparison of those based on the PD test results. Firstly, hydroformed BPPs were compared from manufacturing sequence point of view. Then, the comparisons between the stamped-coated and the coated-stamped BPPs were made. Finally, 1 μm-thick uncoated–coated blank, formed-coated and coated-formed BPPs were compared as best performed coating thickness group. Logarithmic scales were preferred to cover very wide range of corrosion density values in graphs. Statistical significance of PD test results were investigated by means of ANOVA tests as presented in Section 4.

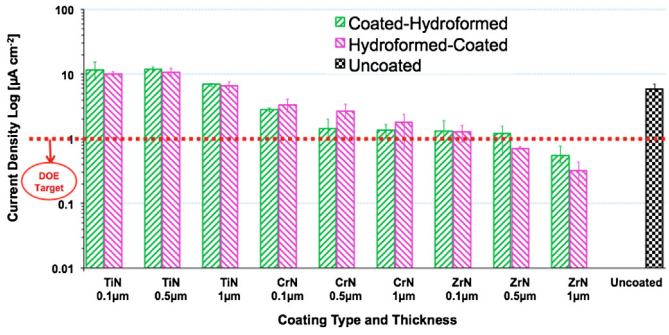

Fig. 4. PD corrosion test results for hydroformed-coated and coated-hydroformed BPPs.

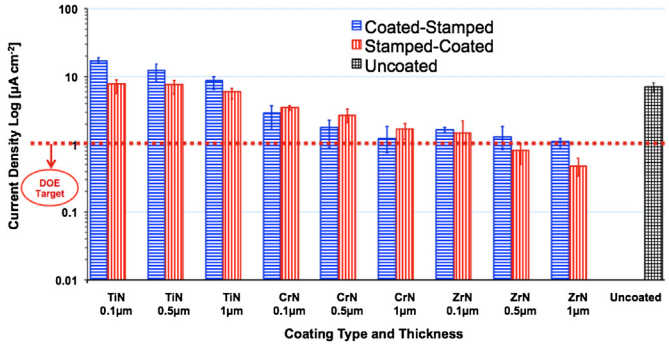

Fig. 5. PD corrosion test results for stamped-coated and coated-stamped BPPs.

3.1.1. *Comparison of hydroformed-coated and coated-hydroformed BPPs*

To reveal the effect of process sequence among the hydroformed samples on corrosion resistance, Fig. 4 was constructed using average I_{corr} values for hydroformed-coated and coated-hydroformed BPPs. It is observed that the ZrN and TiN coatings applied on sheet blanks prior to hydroforming resulted in lowered corrosion endurance for BPPs. For the CrN coating, however; BPPs became more resistant when the sample was coated before forming. From the results shown in Fig. 4, current density values of only three samples were located below the red dashed line, which represents the DOE target. Two of them were coated with 1 μm-thick-ZrN before and after hydroforming process whereas the third one was coated with 0.5 μm-thick-ZrN after hydroforming. Additionally, it was clearly seen that the decrease in coating thickness led to lowered corrosion resistance. Furthermore, uncoated hydroformed samples exhibited lower corrosion densities than the TiN coated samples regardless of forming-coating sequence.

3.1.2. *Comparison of stamped-coated and coated-stamped samples*

Similar to hydroformed samples, the corrosion properties of stamped BPPs had same trend in terms of the forming-coating effect. It was seen that the CrN coated BPP samples corroded severely when coating applied after stamping process. In contrast to hydroformed samples, only two groups of coated after stamping, 0.5 and 1 μm-thick-ZrN coating samples, met the DOE target. As it was experienced in hydroforming case, higher coating thicknesses yielded higher corrosion resistance in both formed-coated and coated-formed cases. TiN coated-stamped BPPs showed worse resistance against corrosion than uncoated BPPs, similar to hydroforming case. Fig. 5 illustrated all these findings.

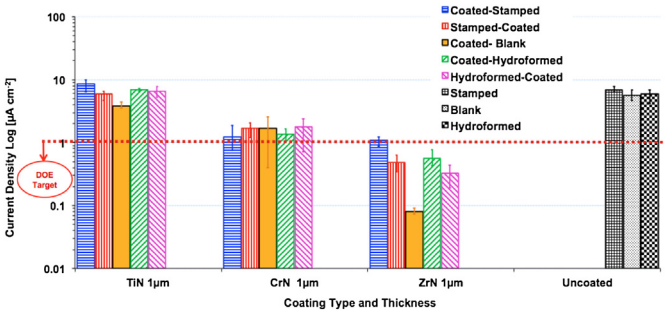

Fig. 6. PD corrosion test results for 1 μm-thick uncoated, coated blanks, and formed BPPs.

3.1.3. Corrosion resistance comparison of uncoated and 1 μm-thick-coated blank, hydroformed, stamped, formed-coated and coated-formed BPPs

Since the samples with 1 μm-thick-coating exhibited the highest level of corrosion resistance, those were further analyzed in terms of the process sequence in Fig. 6. It was observed among all the groups that, blank samples have higher corrosion resistance than other that for other samples. Nevertheless, there was only one coating group, CrN, which broke this trend as blanks, coated with CrN prior to forming were better than the blanks coated with CrN in terms of the corrosion resistance. Overall, applying TiN and ZrN coatings after manufacturing process increased the corrosion resistance of the BPPs, whereas the opposite trend was observed for CrN coating. When forming processes are compared, stamped and then coated BPPs corroded more than their hydroformed BPP counterparts in case of ZrN coating, whereas a corrosion formation was higher when BPPs were shaped via hydroforming method and then coated with CrN and TiN coatings. In general, stamped BPPs resisted less to the corrosive environment when compared to hydroformed BPPs for the case of first coated and then formed groups.

3.2. Potentiostatic (PS) corrosion test results for 1 μm-thick coatings

After assessment of PD test results, blanks and BPPs coated with 1 μm-thick coatings were subjected to further investigation by means of PS corrosion tests. These tests were again conducted with O_2 gas purge to simulate the cathodic side of the PEMFC. During the 3 h-long PS corrosion tests, current density-time data were constructed up to 5000 s as the stabilization took place by then. PS corrosion test results for 1 μm-thick coated, uncoated blanks, hydroformed, stamped, coated-formed, and formed-coated samples are all included in Fig. 7. Fig. 8, on the other hand, shows the PS corrosion test results for 1 μm-thick formed-coated and coated-formed BPPs. Since stabilization level range of coating groups was varied and wide, figures were generated with two or three separate parts showing different ranges.

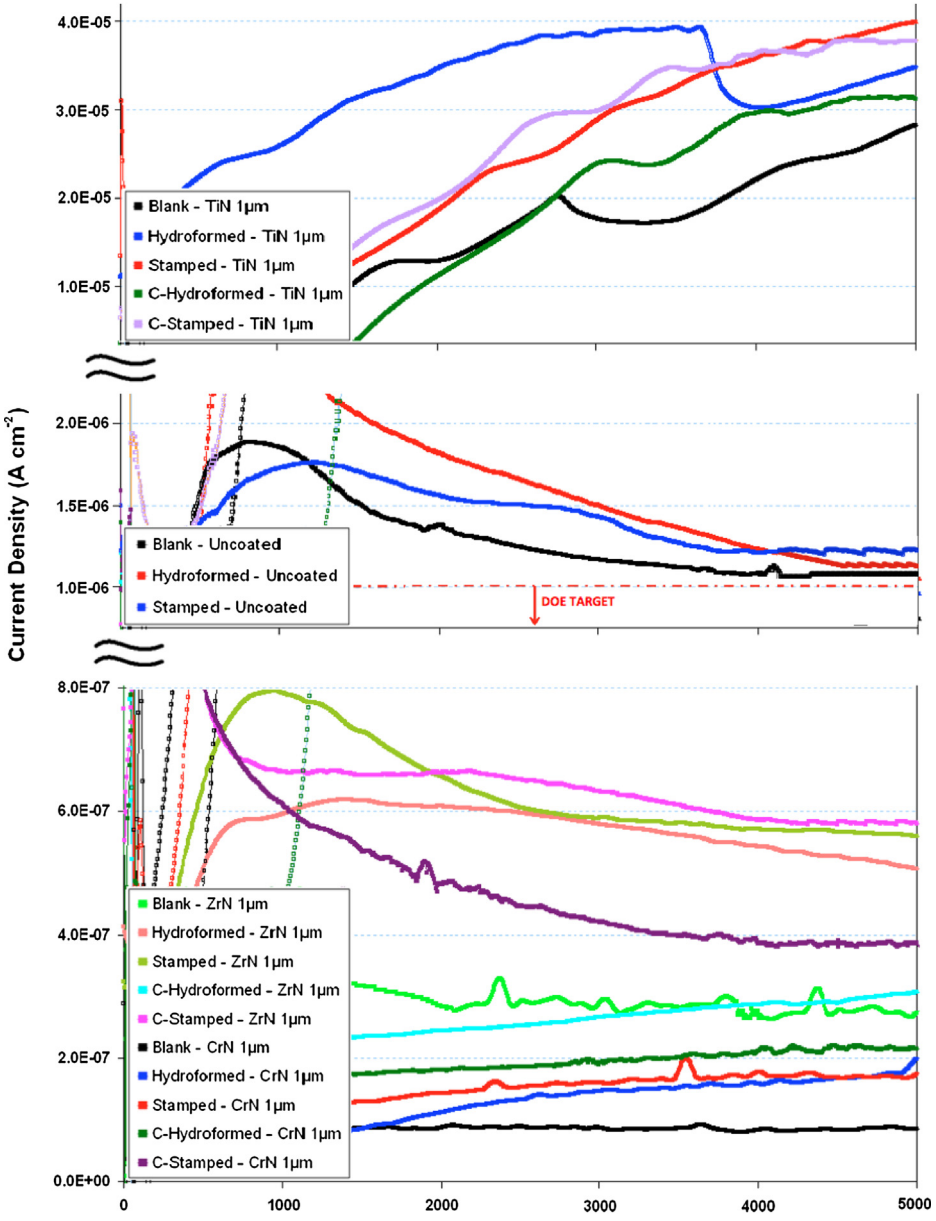

Fig. 7. PS corrosion test results for 1 μm-thick coated, uncoated blanks, and formed BPPs.

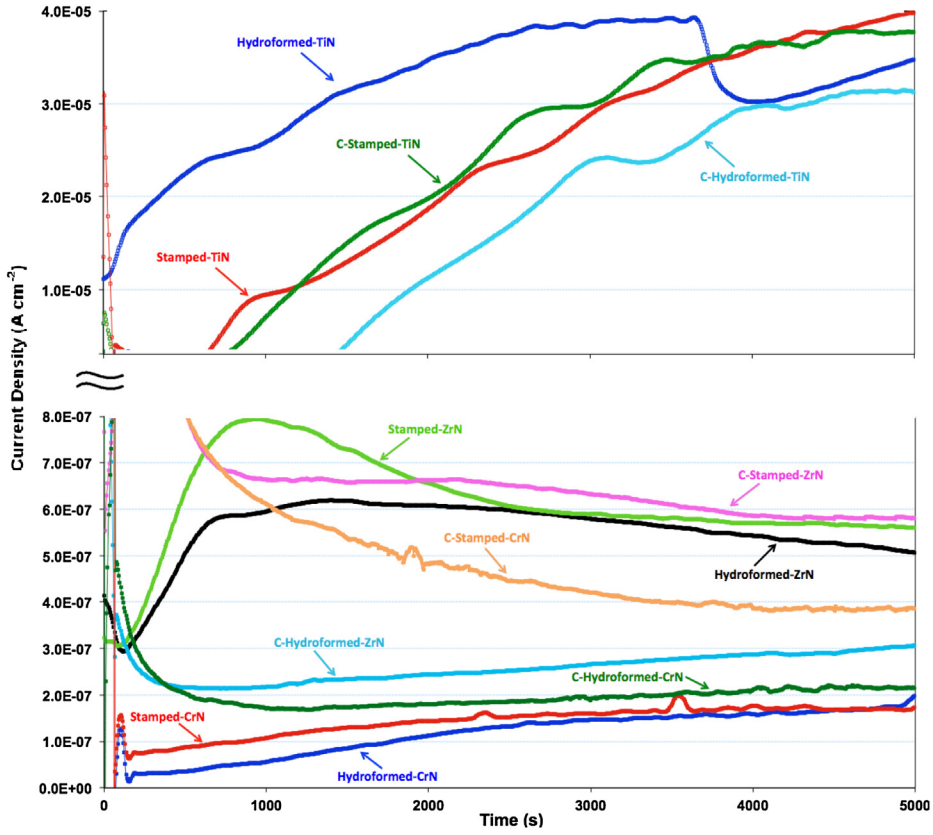

Fig. 8. PS corrosion test results for 1 μm-thick formed-coated, and coated-formed BPPs.

PS test results seen in Figs. 7 and 8 supported the findings obtained from PD tests as discussed in previous sections. TiN coating showed the lowest performance among the tested coatings to corrosion attack. In contrast to PD data, PS tests disclosed the higher performance of CrN coatings than ZrN coating. According to the stabilization levels of their respective curves, both CrN and ZrN coated BPPs satisfied the DOE target. The corrosion resistance performance from high to less was in the order of CrN, ZrN, uncoated blanks, and TiN.

When the effect of forming type on corrosion performance of coatings is evaluated, it was seen that hydroforming process did not negatively affect the corrosion endurance of CrN, ZrN, and TiN coatings as much as the stamping process affected, regardless of the process sequence. Besides, coated blank samples showed the best corrosion resistance in each coating group emphasizing the negative effect of forming processes on the corrosion behavior of BPPs. Unlike the PD test results, hydroforming of plates after ZrN and TiN coatings, and stamping of plates after TiN coating lowered the stabilization level leading to enhanced corrosion resistance according to PS test results. On the other hand, PS test results revealed that CrN and ZrN coated, and then stamped BPPs showed slightly lower corrosion resistance than the stamped first, and then coated BPPs. Another conclusion derived from the PS tests is that coating the sample with CrN before hydroforming process decreased the corrosion endurance of the BPPs. These conclusions are visualized in Fig. 8.

SEM images were acquired from the surface of some coated specimens to observe the forming-coating sequence effect as well as possible corrosion signs before and after PS tests. SEM images of formed-coated and coated-formed BPPs with 1 μm-thick TiN and ZrN coatings are presented in Fig. 9. Intensive macro-defects and pinholes can be noticed on the TiN coated sample before corrosion test in Fig. 9a. Pin-hole type defects seen on the surface of TiN coated samples before the corrosion test were assumed to be sourced from coating process that resulted in lowered corrosion resistance. PVD coating process defects could be decreased, but it could be very difficult to entirely provide defect-free coated surface [20,34]. Moreover, it can clearly be seen that TiN coated sample had intensive corrosion attack after the PS test. No corrosion sign was noticeable after the PS test for the ZrN coating as seen in Fig. 9b.

In the case of coating application prior to forming, coating cracks were easily noticeable for both TiN and ZrN coated samples (Fig. 9c and d) while no such cracks observed on the surface of samples that were coated after manufacturing. These crack formations were undoubtedly caused by the manufacturing process. After corrosion tests, it was noticed that cracks become more definite for both coatings. For the TiN case, cracks were enlarged after the corrosion test as it can be seen in Fig. 9c.

Although significant differences were expected between formed-coated and coated-formed BPPs in terms of the corrosion behavior, coated-formed BPPs exhibited almost the same performance with formed-coated BPPs in most cases based on the PD and PS corrosion test results. Several EDX analyses were performed on ZrN coated BPPs to confirm these results in terms of sequence effect on the corrosion behavior. It can be concluded from Fig. 10a–d that EDX analyses revealed the decreased Zr content on the surface after corrosion tests and manufacturing process, as expected. Nevertheless, these decreases are not significant as the ZrN exhibited the best performance among the tested coatings. Therefore, it can be said that corrosion properties of the BPPs did not change noticeably in regard to forming-coating sequence. Similar conclusion was published by Eriksson et al. who examined the effect of manufacturing process on the coated stainless steel. They reported improved corrosion behavior even though some cracks were observed on the coated surface due to manufacturing process [26].

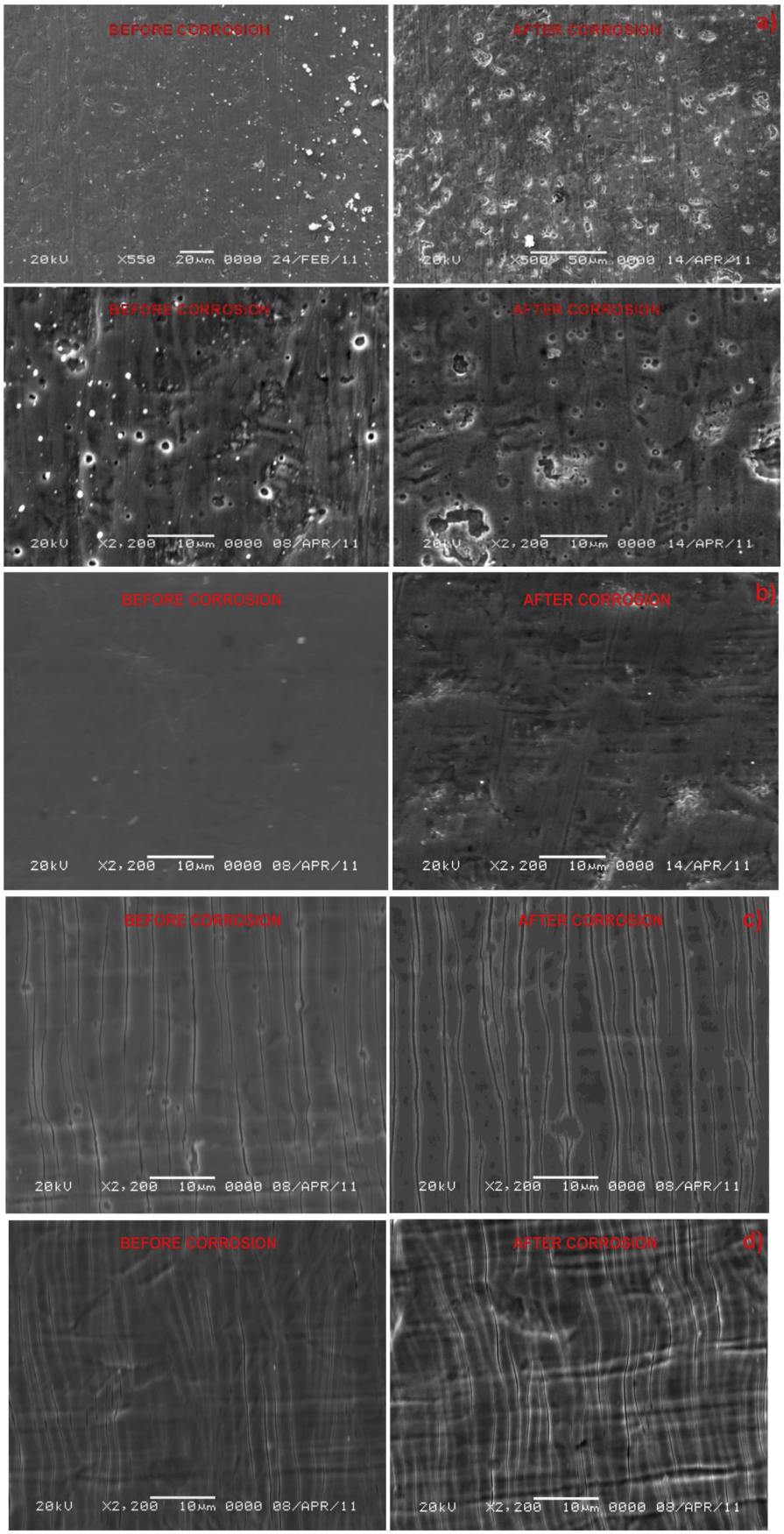

Fig. 9. SEM images before and after PS corrosion tests for 1 μm-thick a) TiN, b) ZrN hydroformed-coated and c) TiN, d) ZrN coated-hydroformed BPPs.

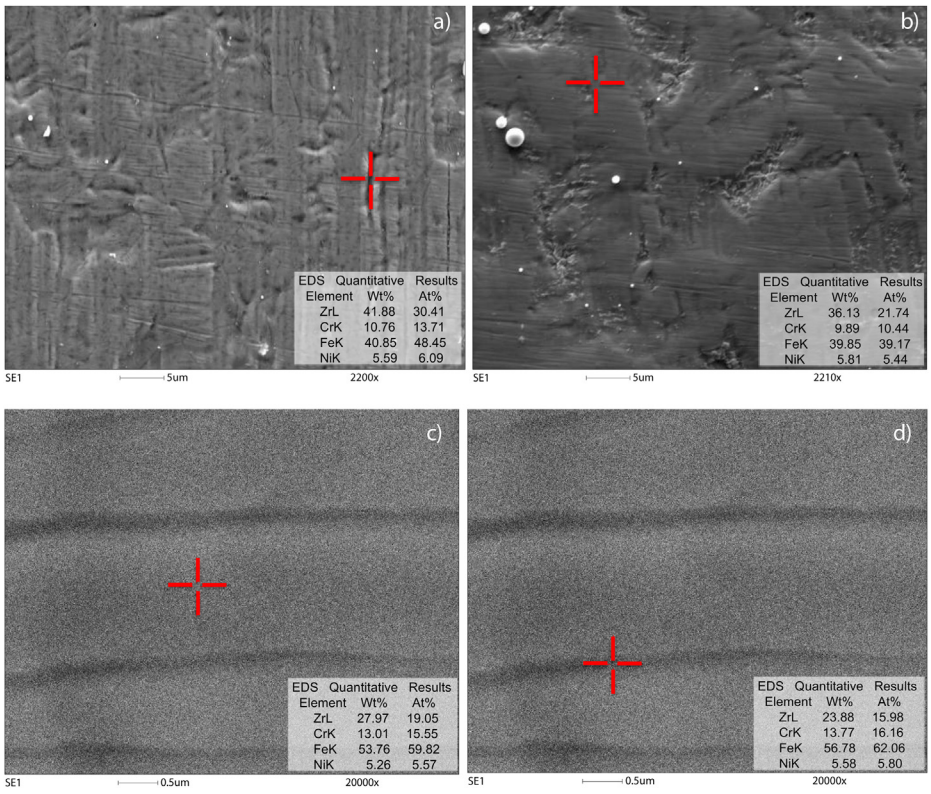

Fig. 10. EDX data for 1 μm-thick ZrN coated BPPs; a) blank-before PS corrosion test, after PS corrosion test b) hydroformed-coated, c) coated-hydroformed from the smooth area, d) coated-hydroformed from the cracked area.

4. Statistical analyses (ANOVA) for corrosion resistance performance

In the light of PD and PS corrosion experiments, following outcomes are reached:

1) ZrN coated BPPs demonstrated higher corrosion resistance than the BPPs coated with other materials.
2) Coating the blank sheet before forming would not influence the BPP's corrosion resistance, considerably.
3) Hydroformed BPPs would resist to corrosion more than its stamped counterparts regardless of the forming-coating sequence.

In order to determine the statistical significance of these outcomes and PD corrosion test results between different test groups, one-way ANOVA (Analysis of Variance) tests were carried out on the averaged I_{corr} values of each group. At least three I_{corr} data from each group were included in analyses. Confidence interval (CI) was selected as 95%. Probability (p) values were obtained by one-way ANOVA analyses value of less than 0.05 stood for significant difference between the compared groups. 1 μm-thick coated, uncoated, blanks, hydroformed, stamped, coated-formed, and formed-coated samples were included in statistical analyses only as these groups exhibited relatively higher corrosion resistance.

First ANOVA analysis yielded p value of 0.000 for the groups including all 1 μm-thick coated samples indicating significant differences from the corrosion resistance perspective. Fig. 11 plots the confidence interval for these groups. Since 1 μm-thick ZrN samples were the best against corrosion, second ANOVA test was performed on this group of which confidence intervals displayed in Fig. 12.

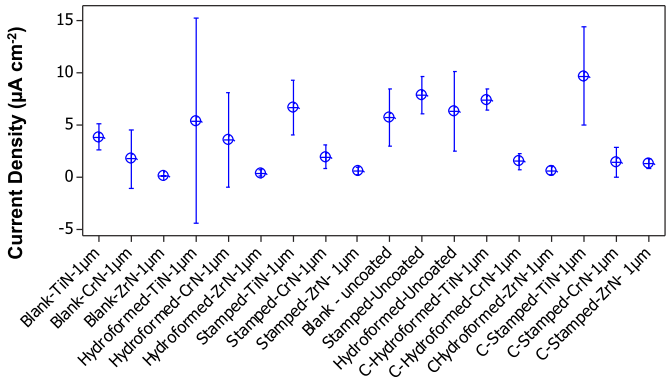

Fig. 11. 95% confidence intervals for 1 μm-thick coated-uncoated blank, hydroformed, stamped, formed-coated and coated-formed BPPs.

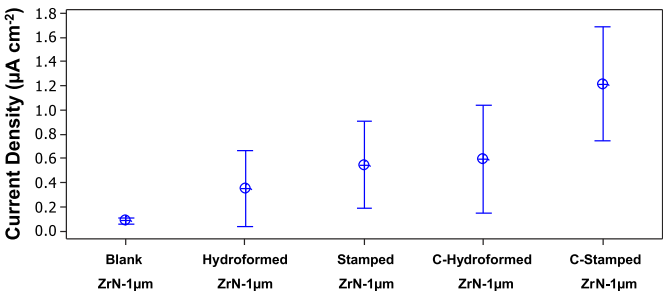

Fig. 12. 95% confidence intervals for 1 μm-thick ZrN coated blank, hydroformed, stamped, coated-hydroformed, and coated-stamped BPPs.

Similar to previous case, differences were found to be significant in this case, too. Further analyses were performed to reveal the statistical significance for manufacturing process, forming-coating sequence, and coating type and thickness in subsequent sections.

4.1. ANOVA analyses for manufacturing process effect

In this part of analyses hydroformed and stamped BPPs with 1 μm-thick ZrN coating were subjected to the ANOVA tests, Probability value of 0.152 obtained from ANOVA analysis for formed-coated samples (stamped-coated vs. hydroformed-coated) yielding that there was no significant difference between hydroforming and stamping processes. Second ANOVA test conducted among the coated-formed samples yielded p-value of 0.015 implying that hydroforming process was found to be decreasing the corrosion current density significantly when compared the stamping process. Thus, hydroforming process would be the promising method for the coated substrate material to form them into the BPP.

4.2. ANOVA analyses for forming-coating sequence effect

Statistical significance tests for process sequence were also performed for hydroformed-coated, coated-hydroformed, and stamped-coated, coated-stamped groups. For hydroforming case with ZrN coating, no significant difference was revealed between two sequences. For stamping case, on the other hand, coated and then stamped BPPs had significantly smaller interval plots than its stamped and then coated counterparts. Results, confirming the previous section, suggested the preference of hydroforming process for coated metals.

In addition, CrN coated BPPs were evaluated with ANOVA since the samples formed after CrN coating gave better corrosion behavior than the samples formed before coating in PD tests. In conclusion, no significant variation was observed for both hydroforming and stamping cases with CrN coating in terms of process sequence as p values of 0.128 and 0.265 were obtained.

4.3. ANOVA analyses for coating type and thickness

ANOVA analysis yielded significant difference ($p = 0.012$) between ZrN and CrN coatings for hydroforming case. Analysis was conducted for the stamping case in both coating sequences. Assessment of results signified that corrosion-preventing feature of ZrN coating was significantly stronger than the CrN coating in all cases with one exception. Corrosion resistances of the CrN and ZrN coatings were found to be not different from each other only when the coating applied on BPP after stamping.

Since hydroformed samples showed slightly higher corrosion resistance, they were tested with ANOVA tests. For 0.1, 0.5, 1 μm-thick ZrN coated hydroformed-coated and coated-hydroformed BPPs. While the effect of coating thickness was not significant for the coated-hydroformed samples, statistical analysis revealed the distinct effect of coating thickness for the hydroformed-coated BPPs.

5. Summary and conclusion

The effects of forming-coating sequence on the corrosion resistance of metallic bipolar plates has been investigated comprehensively through two forming methods, two different process sequence, and three different coatings at three distinct thickness levels as well as two different corrosion test methods.

PD corrosion test results gave the order of corrosion performance of coating materials on BPPs as ZrN > CrN > TiN > Uncoated from the highest to lower for most cases. It was also found that thicker coating increased the corrosion resistance. Coated blank samples possessed highest corrosion resistance almost in all cases. ZrN was the only coating type for both formed-coated and coated-formed groups that met the DOE target. Different from PD test results, CrN coated samples exhibited the highest corrosion resistance while TiN coated samples showed the worst corrosion resistance in PS test results. PS test results also revealed that all BPPs coated with 1 μm-thick CrN and ZrN met the DOE target regardless of forming-coating sequence. PS tests also demonstrated that coated-hydroformed and hydroformed-coated BPPs demonstrated higher corrosion resistance than their stamped counterpart in most cases.

ANOVA tests resulted in insignificant differences for the process sequences in hydroforming case (for ZrN and CrN) and in stamping (for CrN case only). In stamping with ZrN case, however; coated-stamped BPPs had significantly lower corrosion resistance than stamped-coated samples. Consequently, it can be commented that coating the BPP's substrate material before manufacturing process does not always decrease the corrosion resistance of the BPPs.

References

[1] A. Kumar, M. Ricketts, S. Hirano, Journal of Power Sources 195 (2010) 1401–1407.
[2] U.S. Department of Energy, Renewable Energy, Fuel Cell Technologies Program, 2011. Technical Plan – Fuel Cells; also available at: http://www1.eere.energy.gov/hydrogenandfuelcells/mypp/pdfs/fuel_cells.pdf. Last access date: 25.05.2013.
[3] N.M. Sammes, Fuel Cell Technology – Reaching Towards Commercialization, Springer, Germany, 2006.
[4] Y.J. Ren, J. Chen, C.L. Zeng, Journal of Power Sources 195 (2010) 1914–1919.
[5] L.A. Dobrzanski, K. Lukaszkowicz, A. Zarychta, L. Cunha, Journal of Materials Processing Technology 164–165 (2005) 816–821.
[6] H. Yu, L. Yang, L. Zhu, X. Jian, Z. Wang, L. Jiang, Journal of Power Sources 191 (2009) 495–500.
[7] J. Barranco, F. Barreras, A. Lozano, A.M. Lopez, V. Roda, J. Martin, M. Maza, G.G. Fuentes, E. Almandoz, International Journal of Hydrogen Energy 35 (2010) 11489–11498.
[8] M.A. Lucio Garcia, M.A. Smit, Journal of Power Sources 158 (2006) 397–402.
[9] Y. Wang, D.O. Northwood, Journal of Power Sources 163 (2006) 500–508.
[10] Y.J. Ren, C.L. Zeng, Journal of Power Sources 182 (2008) 524–530.
[11] S. Joseph, J.C. McClure, R. Chianelli, P. Pich, P.J. Sebastian, International Journal of Hydrogen Energy 30 (2005) 1339–1344.
[12] M.F. Morks, N.F. Fahim, A. Kobayashi, Journal of Manufacturing Processes 10 (2008) 6–11.
[13] Y. Lee, D. Lim, Current Applied Physics 10 (2010) S18–S21.
[14] S.J. Lee, C.H. Huang, Y.P. Chen, Journal of Materials Processing Technology 140 (2003) 688–693.
[15] H. Jung, S. Huang, P. Ganesan, B.N. Popov, Journal of Power Sources 194 (2009) 972–975.
[16] Y. Yun, International Journal of Hydrogen Energy 35 (2010) 1713–1718.
[17] W. Yoon, X. Huang, P. Fazzino, K.L. Reifsnider, M.A. Akkaoui, Journal of Power Sources 179 (2008) 265–273.
[18] Y.S. Jeong, Y.T. Jeon, H.G. Seong, S.G. Lim, Metals and Materials International 15 (1) (2009) 37–42.
[19] K. Feng, Y. Shen, D. Liu, P.K. Chu, X. Cai, International Journal of Hydrogen Energy 35 (2010) 690–700.
[20] J. Barranco, F. Barreras, A. Lozano, M. Maza, Journal of Power Sources 196 (9) (2011) 4283–4289.
[21] Y. Fu, M. Hou, G. Lin, J. Hou, Z. Shao, B. Yi, Journal of Power Sources 176 (2008) 282–286.
[22] Y. Fu, G. Lin, M. Hou, B. Wu, H. Li, L. Hao, Z. Shao, B. Yi, International Journal of Hydrogen Energy 34 (2009) 453–458.
[23] R. Tian, Journal of Power Sources 196 (3) (2011) 1258–1263.
[24] Y. Wang, D.O. Northwood, Journal of Power Sources 165 (2007) 293–298.
[25] D. Zhang, L. Duan, L. Guo, W. Tuan, International Journal of Hydrogen Energy 35 (2010) 3721–3726.
[26] L. Eriksson, E. Harju, A.S. Korhonen, K. Pischow, Surface & Coatings Technology 53 (1992) 153–160.
[27] M. Li, S. Luo, C. Zeng, J. Shen, H. Lin, C. Cao, Corrosion Science 46 (2004) 1369–1380.
[28] E.A. Cho, U.S. Jeon, S.A. Hong, I.H. Oh, S.G. Kang, Journal of Power Sources 142 (2005) 177–183.
[29] H.Y. Lee, J.W. Choi, G.H. Hwang, S.G. Kang, Metals and Materials International 12 (2) (2006) 147–151.

[30] M.P. Brady, B. Yang, H. Wang, J.A. Turner, K.L. More, M. Wilson, F. Garzon, Journal of Metals 58 (8) (2006) 50–57.
[31] W. Ho, H. Pan, C. Chang, D. Wang, J.J. Hwang, Surface & Coatings Technology 202 (2007) 1297–1301.
[32] H.S. Choi, D.H. Han, W.H. Hong, J.J. Lee, Journal of Power Sources 189 (2009) 966–971.
[33] Y. Wang, D.O. Northwood, Journal of Power Sources 191 (2009) 483–488.
[34] L. Wang, D.O. Northwood, X. Nie, J. Housden, E. Spain, A. Leyland, A. Matthews, Journal of Power Sources 195 (2010) 3814–3821.
[35] Y.J. Ren, C.L. Zeng, Journal of Power Sources 171 (2007) 778–782.
[36] Y. Fu, G. Lin, M. Hou, B. Wu, Z. Shao, B. Yi, International Journal of Hydrogen Energy 34 (2009) 405–409.
[37] K. Feng, Y. Shen, H. Sun, D. Liu, Q. An, X. Cai, P.K. Chu, International Journal of Hydrogen Energy 34 (2009) 6771–6777.
[38] T. Fukutsuka, T. Yamaguchi, S. Miyano, Y. Matsuo, Y. Sugie, Z. Ogumi, Journal of Power Sources 174 (2007) 199–205.
[39] Y. Lee, C. Lee, D. Lim, International Journal of Hydrogen Energy 34 (2009) 9781–9787.
[40] S. Lee, J. Kim, Y. Lee, D. Wee, International Journal of Hydrogen Energy 35 (2010) 725–730.
[41] S. Lee, C. Huang, J. Lai, Y. Chen, Journal of Power Sources 131 (2004) 162–168.
[42] K.H. Cho, W.G. Lee, S.B. Lee, H. Jang, Journal of Power Sources 178 (2008) 671–676.
[43] C. Bai, M. Ger, M. Wu, International Journal of Hydrogen Energy 34 (2009) 6778–6789.
[44] S.B. Lee, K.H. Cho, W.G. Lee, H. Jang, Journal of Power Sources 187 (2009) 318–323.
[45] T. Wena, K. Hou, C. Bai, M. Ger, P. Chien, S. Lee, Corrosion Science 52 (2010) 3599–3608.
[46] L. Yang, H. Yu, L. Jiang, L. Zhu, X. Jian, Z. Wang, Journal of Power Sources 195 (2010) 2810–2814.
[47] K. Feng, Z. Li, X. Cai, P.K. Chu, Surface & Coatings Technology 205 (2010) 85–91.
[48] A. Pozio, R.F. Silva, A. Masci, International Journal of Hydrogen Energy 33 (2008) 5697–5702.
[49] S. Hong, K.S. Weil, Journal of Power Sources 168 (2007) 408–417.
[50] Metals HandbookProperties and Selection: Irons and Steels, ninth ed., vol. 1,, American Society for Metals, Ohio, USA, 1978.
[51] E. Dur, Ö.N. Cora, M. Koç, International Journal of Hydrogen Energy 36 (2011) 7162–7173.
[52] L. Peng, X. Lai, D. Liu, P. Hu, J. Ni, Journal of Power Sources 178 (2008) 223–230.
[53] P.J. Hamilton, B.G. Pollet, Fuel Cells 4 (2010) 489–509.
[54] J. Kim, B.M. Son, B.S. Kang, S.M. Hwang, H.J. Park, Journal of Materials Processing Technology 153-154 (2004) 550–557.
[55] B.-S. Kang, B.-M. Son, J. Kim, International Journal of Machine Tools & Manufacture 44 (2004) 87–94.
[56] M. Li, L. Zhang, S. Wang, S.J. Hu, Journal of Fuel Cell Science and Technology 5 (2008) 1–8, 011014.
[57] F. Dundar, E. Dur, S. Mahabunphachai, M. Koç, Journal of Power Sources 195 (2010) 3546–3552.
[58] M. Koç, S. Mahabunphachai, F. Dundar, ECS Transactions 25 (1) (2009) 1773–1782.
[59] E. Dur, Ö.N. Cora, M. Koç, Journal of Power Sources 196 (2011) 1235–1241.
[60] S. Mahabunphachai, Ö.N. Cora, M. Koç, Journal of Power Sources 195 (2010) 5269–5277.
[61] Y. Wang, D.O. Northwood, Electrochimica Acta 52 (2007) 6793–6798.